Since January 2020 Elsevier has created a COVID-19 resource centre with free information in English and Mandarin on the novel coronavirus COVID-19. The COVID-19 resource centre is hosted on Elsevier Connect, the company's public news and information website.

Ultrasound in Med. & Biol., Vol. 46, No. 9, pp. 2530–2545, 2020

0301-5629/$ - see front matter

https://doi.org/10.1016/j.ultrasmedbio.2020.05.012

● *Clinical Note*

A REVIEW OF EARLY EXPERIENCE IN LUNG ULTRASOUND IN THE DIAGNOSIS AND MANAGEMENT OF COVID-19

LAITH R. SULTAN, and CHANDRA M. SEHGAL
Department of Radiology, University of Pennsylvania, Philadelphia, Pennsylvania, USA

(*Received* 17 *April* 2020; *revised* 12 *May* 2020; *in final from* 15 *May* 2020)

Abstract—A novel coronavirus (2019-nCoV) was identified as the cause of a cluster of pneumonia in Wuhan, China, at the end of 2019. Since then more than eight million confirmed cases of coronavirus disease 2019 (COVID-19) have been reported around the globe. The current gold standard for etiologic diagnosis is reverse transcription–polymerase chain reaction analysis of respiratory-tract specimens, but the test has a high false-negative rate owing to both nasopharyngeal swab sampling error and viral burden. Hence diagnostic imaging has emerged as a fundamental component of current management of COVID-19. Currently, high-resolution computed tomography is the main imaging tool for primary diagnosis and evaluation of disease severity in patients. Lung ultrasound (LUS) imaging has become a safe bedside imaging alternative that does not expose the patient to radiation and minimizes the risk of contamination. Although the number of studies to date is limited, LUS findings have demonstrated high diagnostic sensitivity and accuracy, comparable with those of chest computed tomography scans. In this note we review the current state of the art of LUS in evaluating pulmonary changes induced by COVID-19. The goal is to identify characteristic sonographic findings most suited for the diagnosis of COVID-19 pneumonia infections. (E-mail: lsultan@pennmedicine.upenn.edu) **© 2020 Published by Elsevier Inc. on behalf of World Federation for Ultrasound in Medicine & Biology.**

Key Words: **COVID-19, coronavirus, lung imaging, lung ultrasound, pneumonia, point of care ultrasound (POCUS).**

INTRODUCTION

Coronavirus disease 2019 (COVID-19) is an infectious disease caused by severe acute respiratory syndrome coronavirus 2 (2019-nCoV), (World Health Organization 2020a). This disease was first identified in 2019 in Wuhan, China, and has since spread globally, resulting in the ongoing 2020 coronavirus pandemic (Hui et al. 2020; World Health Organization 2020b).The standard method of diagnosis is by reverse transcription–polymerase chain reaction from a nasopharyngeal swab (Van Doremalen Neeltje et al., 2020), in addition to assessment of clinical symptoms, risk factors and imaging features indicative of pneumonia (Practice 2020; Velavan and Meyer 2020). Imaging features are determined largely by chest computed tomography (CT) for diagnosis and during follow-up (Li et al., 2020a; Wang et al. 2020). Although chest X-ray is typically the first-line imaging mode used for patients with suspected COVID-19, it has less sensitivity than chest CT scan (Wong et al. 2019).

While chest CT has excellent ability to detect COVID-19 lung changes (Li et al., 2020b; Wang et al. 2020), it has the disadvantages of large radiation exposure, lack of portability for bedside imaging and risk of cross infections between patients. As a result, a significant interest has emerged in the use of lung ultrasound (LUS) as an alternative first-line imaging modality. LUS use has evolved over the years in the diagnosis of severe lung diseases in critically ill patients, complementing conventional assessment methods and other imaging modalities for the lungs (Bouhemad et al. 2007; Bakhru and Schweickert 2013; Saraogi 2015; Lichtenstein and Malbrain 2017; Arbelot et al. 2020). LUS is cost-effective, readily available at bedside, real-time and free of radiation hazards.

In the current COVID-19 pandemic, LUS is being used in emergency rooms for triaging symptomatic patients for pneumonia before hospital admission, monitoring patients with pneumonia-related lung findings, managing ventilation and weaning for intensive-care–unit patients and evaluating the effects of antiviral medications (Buonsenso et al. 2020a,

Address correspondence to: Laith R. Sultan, University of Pennsylvania, Department of Radiology, 3620 Hamilton Walk, Philadelphia, PA 19104. E-mail: lsultan@pennmedicine.upenn.edu

2020b; Denina et al. 2020; Huang et al. 2020; Inchingolo et al. 2020; Kalafat et al. 2020; Lomoro et al. 2020; Musolino et al. 2020; Peng et al. 2020; Poggiali et al. 2020; Soldati et al. 2020; Thomas et al. 2020; Tung-Chen 2020; Yasukawa and Minami 2020). This note is aimed at the practitioners in various subspecialties of allied health. It summarizes the current state of the art of LUS and its emerging application for the diagnosis and management of COVID-19.

THE BASICS OF NORMAL LUNG ULTRASOUND

The diagnostic findings of LUS imaging are based on the relative amounts of air and fluid present in the lung as determined by acoustic impedance (Z), a measure of the resistance of particles in a medium to mechanical vibrations (Miller 2016). The value of Z increases in proportion to the density of the tissue and to ultrasound velocity in the tissue. When ultrasound energy strikes a large, flat boundary between two media of different impedances, a part of the sound energy is reflected as an echo, and the remaining energy is transmitted across the boundary. The greater the difference in Z between the two media, the stronger the reflection and the weaker the transmission through the tissue. During LUS scanning the transducer is usually placed longitudinally, perpendicular to the ribs over intercostal space. The ultrasound beam propagates through skin, subcutaneous tissue and muscles to reach boundaries between soft tissue and rib and between visceral pleura and lung air. At the soft tissue−rib boundary the ultrasound wave is almost totally reflected back owing to large acoustic impedance, and the rib appears as a convex white (hyperechoic) bow-like line followed by posterior acoustic shadow beyond the boundary. Similarly, at the visceral pleura−lung air boundary, approximately 0.5 cm deeper and between the upper and lower ribs in adults, almost all (>99.9%) of the incident ultrasound is reflected back, leaving little to image beyond the pleura (Aldrich 2007; Bouhemad et al. 2007; Arbelot et al. 2020). The result is that in a normally aerated lung, the only detectable structure is the pleura, visualized as a highly hyperechoic horizontal line (pleural line; Fig. 1). This boundary appears as white band (lung/pleural line) measuring up to 2 mm (Koegelenberg et al. 2012). Movement of visceral pleura over parietal pleura produces lung sliding, which makes this white band appear dynamic. Lung sliding is the visualization of a regular rhythmic movement synchronized with respiration that occurs between the parietal and visceral pleura that are either in direct apposition or separated by a thin layer of intrapleural fluid. Lung sliding is an indicator of ventilation in the inspected area.

Beyond this pleural line in a normally aerated lung, artifacts are seen in the images (Lichtenstein et al. 2009). These are reverberation artifacts, produced by the bouncing of echo between the pleural line and probe. In this context, the scattering of ultrasound waves produces artifacts on the images: horizontal reverberations of the pleural line (A-lines; Fig. 1). These artifacts usually appear as motionless, regularly spaced (equal to the

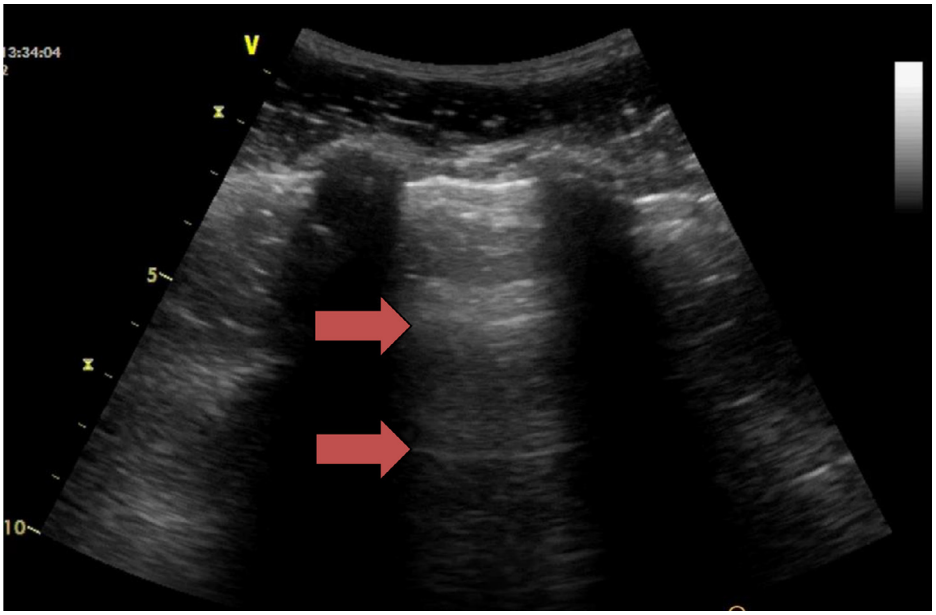

Fig. 1. Normal aerated lung ultrasound showing the horizontal reverberation artifacts (A-lines) of the pleural line (*red arrows*). The characteristic appearance of two ribs and the pleural line in between is often referred to the "bat sign." Reprinted with permission from Miller (2016).

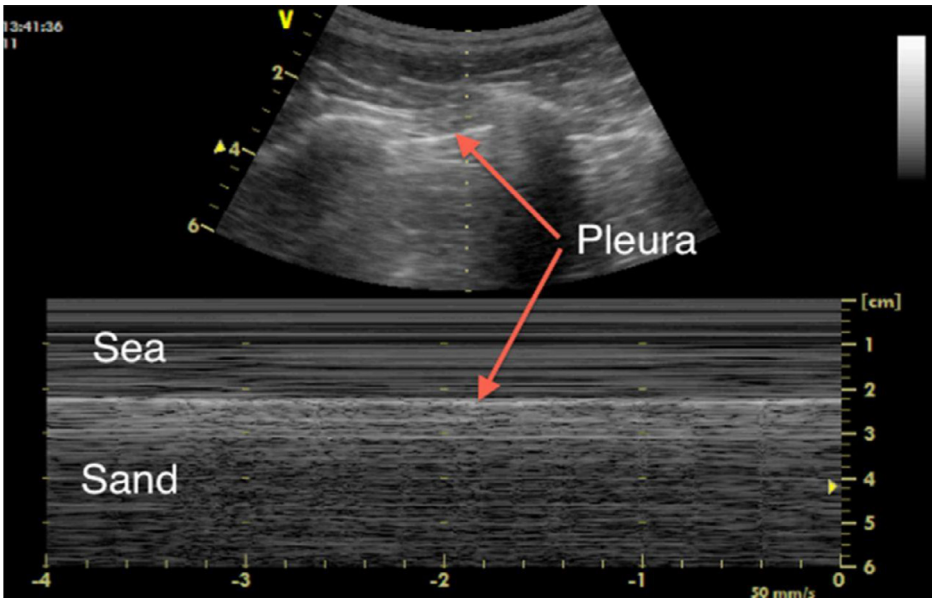

Fig. 2. M-mode image for a normal lung, demonstrating lung sliding (the "seashore sign"). Reprinted with permission from Miller (2016).

distance between the skin and the pleural line) and gradually fading horizontal white lines which resemble pleural lines. The extent of these artifacts varies depending on the ratio of air and fluid in the lung.

When the probe is positioned in the intercostal space, the pleural line and A-lines are visible in the images. When the probe is positioned longitudinally, the ribs cause posterior shadowing, but the pleural line and A-lines between the ribs are still clearly observable along with the shadowing. The characteristic appearance of two ribs with a pleural line in between is often referred to as the "bat sign" (Fig. 1).

While B-mode ultrasound is the major mode used for lung imaging, time–motion mode (M-mode)—the motion display of the ultrasound wave over time along a chosen ultrasound line—can provide extra diagnostic information. In M-mode, tissue structures up to the parietal pleura appear as horizontal lines, and tissues beyond the pleura exhibit a sandy pattern characteristic of lung sliding, called the seashore sign (Fig. 2). The presence of pleural lines, lung sliding, A-lines in 2-D and the seashore sign in M-mode indicate an aerated lung (Lichtenstein and Mezière 2008; Lichtenstein et al. 2009).

Although there are a number of protocols for scanning the lungs described in the literature, one of the most commonly used is the BLUE protocol (Lichtenstein and Mezière 2008; Miller 2016), because it is quick and simple and provides high diagnostic accuracy. As illustrated in Figure 3, two hands are applied side by side (without thumbs) over the anterior chest with the wrists in the anterior axillary line and the upper little finger resting along the clavicle. The lower little finger is aligned with

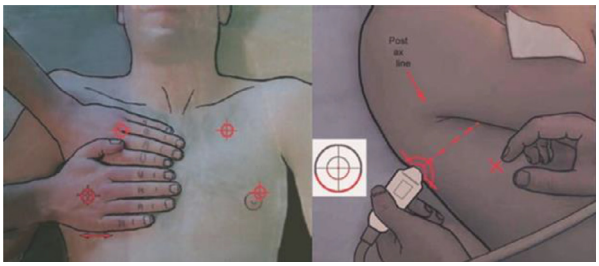

Fig. 3. Probe positioning according to the BLUE protocol. Reprinted with permission from Miller (2016).

the lower border of the lung (the phrenic line). For each point, the probe is aligned vertically to the skin surface, looking into the lung, with the left of the screen cephalad and the right caudad. All views are longitudinal and not transverse. Three points are obtained: the *upper anterior point,* corresponding to the base of the middle and ring fingers on the upper hand, which lies over the upper lobe; the *lower anterior point,* the middle of the palm on the lower hand (close to the nipple on a man), which lies over the middle or lingular lobe; and the *posterolateral point,* which lies behind the posterior axillary line over the lower lobe.

LUNG ULTRASOUND FEATURES RELATED TO PATHOLOGICAL CHANGES

When the ratio between air and tissue, fluid or other biological components is reduced, the lung no longer presents as an almost complete specular reflector. Hence,

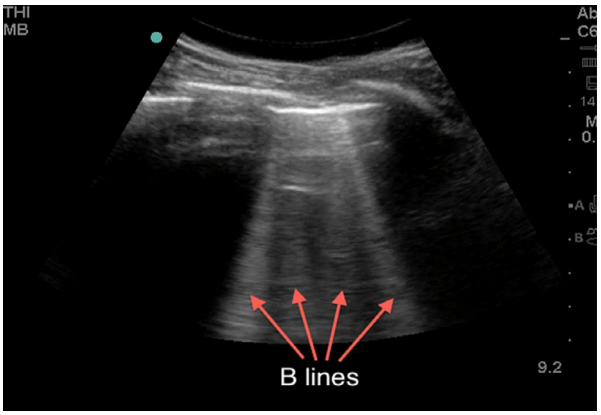

Fig. 4. Lung ultrasound image showing vertical artifacts (B-lines) indicating the presence of a pathology associated with increase in lung tissue density. Reprinted with permission from Miller (2016).

various types of localized vertical artifacts appear in the ultrasound images owing to the alterations of the subpleural tissue. These vertical artifacts of different shapes and lengths, often referred to as B-lines (Fig. 4), occur when the lung loses normal aeration but is not completely consolidated (Saraogi 2015; Miller 2016). The reasons for these lines are not completely understood but are multifactorial; possibly they represent acoustic channels of varying shapes and sizes generated by altered peripheral air−tissue space caused by pathologic conditions. In essence, B-lines define discrete laser-like vertical hyperechoic reverberation artifacts that arise from the pleural line extending to the bottom of the screen without fading, moving synchronously with lung sliding. These B-lines are often visible in the images and are indications of abnormality, but they are not specific to a single pathology. However, clinical information accompanying imaging can help to distinguish different pathologies represented by B-lines. For example, B-lines in a pregnant woman's lung sonogram, forming a pattern of vertical lines radiating into the lung tissue, can indicate severe pulmonary edema complicating previously undiagnosed pre-eclampsia (Zieleskiewicz et al. 2013). This presentation would not be associated with pulmonary fibrosis or chronic obstructive pulmonary disease, as they are typical pathologies of advanced age. Similarly, cardiogenic pulmonary edema is characterized by regular, laser-like, bright B-lines, particularly evident bilaterally on the lung bases (owing to the gravitational effect on cardiogenic edema), without spared areas, and the pleural line is regular (Dietrich et al. 2016). Conversely, in inflammatory lung disease such as viral pneumonia (including early stages of COVID-19), the pleural line is usually irregularly thickened (blurred), and with a characteristic distribution: monofocal or multifocal, patchy or inhomogeneous involvement, surrounded by spared areas and with no gravitational distribution. A few B-lines (fewer than three in the field of view) can often be found under normal circumstances, especially in the elderly and around the base of the lungs.

Another well-known phenomenon linked to increased subpleural lung density in the absence of consolidated tissue is the coalescence of many vertical artifacts to form more extended echogenic patterns, either with recognizable individual artifacts or with individual artifacts fused in a single homogeneous subpleural echogenic area (white lung; Koegelenberg et al. 2012; Miller 2016). As the subpleural density approaches that of solid tissue (~1 g/mL), consolidations appear in the image. When the density of the peripheral (subpleural) lung parenchyma increases but not to the extent that it reaches a consolidative state—as often happens in acute respiratory distress syndrome (ARDS), including COVID-19-induced ARDS—ultrasound examination shows a white area in which no horizontal reverberations (A-lines) nor separated B-lines are visible (Fig. 5). This representation is commonly called "ultrasonographic white lung." On the other hand, when there is a complete consolidation of the lung, the echo structure of the lung itself becomes visible with characteristic air bronchogram, representing the air inside alveoli or bronchi surrounded by inflammation or pus; and the pleural lines are completely obscured (Fig. 5).

LUNG ULTRASOUND APPLICATION IN COVID-19 PATIENTS

This section presents LUS findings from a number of COVID-19 cases reported from around the globe (Buonsenso et al. 2020a, 2020b; Denina et al. 2020; Huang et al. 2020; Inchingolo et al. 2020; Kalafat et al. 2020; Lomoro et al. 2020; Musolino et al. 2020; Peng et al. 2020; Poggiali et al. 2020; Soldati et al. 2020; Thomas et al. 2020; Tung-Chen 2020; Yasukawa and Minami 2020). Our literature

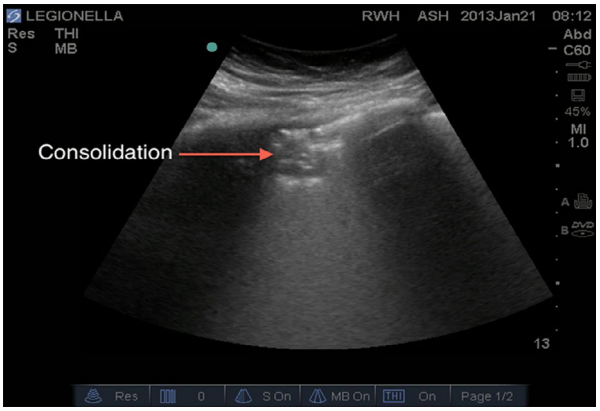

Fig. 5. Lung ultrasound image showing a small anterior consolidation area with indistinct margins (*red arrow*). Reprinted with permission from Miller (2016).

searches on PubMed and Google Scholar used the keywords "coronavirus," "COVID-19," "lung ultrasound" and "imaging findings for COVID-19." The search resulted in 11 case reports and studies published in the last 2 mo for adult cases of COVID-9: two from China, six from Italy, one from Japan, one from Canada and one from Turkey. Each study contained a different number of cases, ranging from one to 22. Additionally, we include LUS findings reported by an emergency medicine physician in Spain who was infected with COVID-19 and recovered. We also looked at LUS findings reported in children confirmed to have COVID-19 in two studies from Italy. Our aim is to summarize the predominant LUS findings of COVID-19 pneumonia/ARDS to define the patterns characteristic of COVID-19. Clinically, although a small percentage of cases (<10%) will show severe symptoms and complications from pneumonia-like changes in the lung, severe COVID-19 cases may rapidly progress to ARDS, resulting in respiratory failure, septic shock or multiorgan failure (Yang et al. 2020). Therefore, it is important to assess the role of LUS as a tool for early detection of lung changes and for monitoring patient prognosis longitudinally throughout the disease duration and recovery.

Histopathologic studies for patients with COVID-19 show inflammatory pulmonary changes characterized by the presence of alveolar edema, reactive alveolar epithelial hyperplasia, prominent proteinaceous exudates, vascular congestion and clusters with fibrinoid material, multinucleated giant cells and fibroblastic proliferation (fibroblast plugs). Reparative processes with pneumocyte hyperplasia and interstitial thickening can occur. The advanced phases show gravitational consolidations similar to those of ARDS. In these phases we can see hemorrhagic necrosis, alveolar congestion, edema, flaking and fibrosis. Accumulation of fluid in subpleural interstitial and alveolar spaces alters the air−fluid ratio, producing B-lines which range from focal to multifocal to fused according to the stage of the disease, until the late stages, where consolidation of the lung is observed. Table 1 summarizes typical lung ultrasonography findings reported from patients with COVID-19.

COVID-19 experience from China

A medical team from Xi'an Chest Hospital (Huang et al. 2020) reports LUS findings from 20 patients with confirmed COVID-19. Ultrasound exams were conducted using a 3−17 MHz high-frequency linear-array transducer and 1−8 MHz convex array probe in six zones per lung within 12 lung scanning regions (approach discussed later). The rationale for using the high-frequency linear array was its ability to clearly display the lung morphology and changes of subpleural lesions, as well as the changes of air and water contents in consolidated peri-pulmonary tissues. Furthermore, high-frequency imaging revealed air bronchogram signs in unconsolidated lung tissues caused by intra-pulmonary hemorrhage, which is of high significance in detecting peri-pulmonary lesions.

In the 12-area examination, each lung was divided by anterior and posterior axillary lines into three areas: anterior, lateral and posterior. The two lobes of the lungs were divided into six areas each. The three dots used in the BLUE protocol (Lichtenstein and Mezière 2008; Miller 2016) served as the boundary (Fig. 3) and were perpendicularly connected with the anterior and posterior axillary lines to the spine point to divide each lung into upper and lower fields. The lesion sites were marked and identified by an R/L 1:6 subdivision-labeling method, where *R* and *L* represent the right and left lungs and the numerals 1 through 6 designate (1) anterior upper area, (2) anterior lower area, (3) axillary upper area, (4) axillary lower area, (5) posterior upper area and (6) posterior lower area. Observations included whether the pleural line was smooth, continuous or interrupted; the distribution, number and fusion of B-lines in the peri-pulmonary area of both lungs; the echo, location, shape and range of peri-pulmonary lesions; whether there was air bronchogram sign, or air bronchogram sign in the consolidation; and blood flow in the consolidation.

All 20 COVID-19 patients reported had a history of risk factors, suggestive symptoms and positive blood testing. The pathologic status of reported patients ranged from mild focal to severe bilateral interstitial patterns and lung consolidation. In terms of LUS findings, most cases showed a patchy distribution of interstitial artifactual signs such as single or confluent vertical artifacts and small white-lung regions. Subsequently these patterns extend to multiple areas of the lung surface, and further evolution of the disease is represented by the continued patchy appearance of small subpleural consolidation along with associated areas of white lung. These conditions present as fused and scattered B-lines (waterfall signs) in the imaging. The pleural line is unsmooth, discontinuous or interrupted. The subpleural lesions show patchy strips and nodule consolidation, in which the air bronchogram sign can be seen. The involved interstitial tissues show obvious thickening and edema, the pleura shows localized thickening and there is localized pleural effusion around the lesions. More consolidations with or without air bronchograms, especially in a gravitational position, and their increasing extension along the lung surface indicate disease progression to a phase of respiratory insufficiency requiring invasive ventilator support. It is observed that pleural effusions are uncommon. During the recovery phase of COVID-19 the reappearance of A-lines was observed.

In COVID-19 patients, the lesions were mostly located in the posterior fields of both lungs. Multiple

Table 1. Summary of lung ultrasound (LUS) findings reported from COVID-19 patients in different studies around the globe

Study	Findings	Scanning protocol	Demographic characteristics/other information
Huang et al. (2020): Case report	• Discontinuous or continuous/fused B-lines common → 37.9% • Pleural line unsmooth and rough → 15% • Multiple small, patchy subpleural consolidations → 22.1% • Air bronchograms → 15.4% • Local pleural effusions around the lung lesions → 18.8% • Pleural thickening 1−2 mm → 14.6% • Poor blood flow in lesions (unlike other findings, not assessed in all patients) → 94.3% • Right and left posterior inferior lung involvement → 75% each; posterior superior → 50%	• Performed with two transducers (a 3−17 MHz high-frequency linear-array transducer and 1−8 MHz convex array) • Thorax was scanned in 12 lung areas • In case of multiple lesions in both lungs, the largest lesion was selected for observation	• Cases: 20 • Location: China • Sex: 11 men, 9 women • Age: Range = 27−81 y; median = 44.5 y (3 cases ≥ 65 y, 17 cases <65 y) • Risk factors: History of travel to Wuhan
Peng et al. (2020): Letter to editor	• Thickening of the pleural line with pleural-line irregularity • B-lines in a variety of patterns including focal, multifocal and confluent • Consolidations in a variety of patterns including multifocal small, non-translobar and translobar with occasional mobile air bronchograms • Appearance of A-lines during recovery phase • Pleural effusions uncommon	• Thorax was scanned in 12 lung areas • No information about transducers used	• Cases: 20 • Location: China • Sex: No details • Age: No details • Risk factors: No details
Lomoro et al. (2020): Original research	• Thickened pleural line → 13.6% • Various patterns of B-lines → 100% • Consolidation → 27.3% • Pleural effusion → 4.5% • A-lines → 4.5%	• Bedside ultrasound was performed in the emergency department using linear or convex probes • No information about scanning protocol	• Cases: Total 58 patients in the study, 22 with ultrasound images • Sex: 36 men, 22 women • Age: Range = 18−98 y
Poggiali et al. (2020): Letter to editor	• Thickening of pleural line, irregular pleural line • B-lines focal and confluent • Consolidations including air bronchograms • Not that many pleural effusions • A-lines during recovery	• No information	• Cases: 12 • Location: Italy • Sex: 9 men, 3 women • Age: Mean ± standard deviation = 63 ± 13 y
Soldati et al. (2020): Clinical letter	• Typical vertical pneumogenic large artifacts (B-lines) originating from the pleural line or from small, blurred subpleural consolidations • Pleural line interrupted by more visible yet small consolidations • White lung	• Convex transducer used • Scanning protocol in 16 areas, intercostal scans	• Cases: 2 • Location: Italy • Sex: No details • Age: No details
Buonsenso et al. (2020a): Case report	• Bilateral irregular pleural line with small subpleural consolidations • Areas of white lung and thick, confluent and irregular vertical artifacts (B-lines)	• Performed with a portable convex probe (3.5 MHz), wirelessly connected with a tablet • Thorax was scanned in 12 lung areas	• Case: 1 • Location: Italy

(*continued on next page*)

Table 1 (***Continued***)

Study	Findings	Scanning protocol	Demographic characteristics/other information
	• Spared areas present bilaterally		• Sex: Male • Age: 52 y
Buonsenso et al. (2020b): Case report	• Irregular pleural lines and vertical artifacts (B-lines) in all cases • Patchy areas of white lung in 2 cases	• No information about scanning protocol	• Cases: 4 • Location: Italy • Age: Median = 37 y; range = 31–42 y; gestational ages = 24, 38, 17 and 35 wk • 2 vaginal deliveries, 2 cesarean with normal outcomes
Inchingolo et al. (2020): Clinical opinion	• Diffuse hyperechoic vertical artifacts • Thickened pleural line • White lung with patchy distribution on 3 out of 14 predetermined scan sites	• Wireless ultrasound probe convex color Doppler C05 C with a frequency of 3.5 MHz • 14 scanning areas (3 posterior, 2 lateral and 2 anterior) along paravertebral, midaxillary and hemiclavear lines • Performed with the first operator scanning the patient with the probe and the second operator outside the room evaluating images and videos in real time, wirelessly, in order to reduce operator exposure to contamination	• Case: 1 • Location: Italy • Gender: Female • Pregnant woman (23 wk) admitted for fever and cough
Tung-Chen (2020): Personal report	• Early signs: Small bilateral pleural effusion, thickened pleural line and basal B-lines • During disease progression: Plural thickening and subpleural consolidations • Later: Effusion resolved, as subpleural consolidations spread bilaterally on both posterior lower lobes	• Used portable ultrasound device (Butterfly IQ)	• Case: 1 • Location: Spain • Sex: Male • Age: 35 y
Yasukawa and Minami (2020): Original article	• Characteristic five or more B-lines in all cases • White lung in 5 cases • 3 or 4 B-lines between 2 ribs in 2 cases • Thick, irregular pleural lines present in all cases	• Performed using a phased-array transducer • Performed along the midclavicular line in the bilateral anterior chest wall and the scapular line and interscapular regions in the posterior chest wall at the bedside by an experienced physician while the patients were sitting up • The transducer was covered with a probe cover, and the transducer and tablet/portable ultrasound device were cleaned with disinfectant wipes after each use	• Cases: 10 • Location: Japan • Sex: 7 men, 3 women • Age: Mean 53 y; range = 31–79 y
Thomas et al. (2020): Clinical image	• Pleural thickening • Subpleural consolidation • Multifocal B-lines	• No information about scanning device or protocol	• Case: 1 • Location: Canada • Sex: Female • Age: 64 y

(*continued on next page*)

Table 1 (*Continued*)

Study	Findings	Scanning protocol	Demographic characteristics/other information
Kalafat et al. (2020): Case report	• Thick B-lines bilaterally, located in the basal posterior lung segments	• No information about scanning device or protocol	• No travel history • Case: 1 • Location: Turkey • Sex: Female • Age: 32 y • 35 wk pregnant
Musolino et al. (2020): Clinical note	• Vertical artifacts → 70% • Pleural irregularities → 60% • Areas of white lung → 10% • Subpleural consolidations → 10% • No cases of pleural effusions found	• Performed with a wireless pocket device connected to a probe, placed in single-use plastic covers • Performed with patients in the sitting position, and all lung areas were scanned, as suggested by Soldati et al. (2020)	• Cases: 10 • Location: Italy • Age: Median = 11 y; range = 4–15 y • Sex: 3 girls, 7 boys • Previous medical history was unremarkable in all cases
Denina et al. (2020): Research brief	• Confluent B-lines in 5 cases • Subpleural consolidations in 2 cases	• Performed during routine medical examination, with a linear-array transducer at 7.5–13 MHz	• Cases: 8 • Location: Italy • Age: Median = 4.2 y; Range = 0.2–10 y • Sex: 3 girls, 5 boys

discontinuous or continuous fused B-lines (waterfall sign) under the pleural line (Fig. 6a), or diffused B-lines (white-lung sign) with disappearing A-lines (Fig. 6b), were observed. The B-lines had blurred edges and no bifurcation signs. The origin point of the subpleural lesion was more obtuse (convex array probe) compared with that of B-lines of pulmonary edema, as shown in Figure 6c. High-frequency ultrasound showed that the pleural line was unsmooth and rough (Fig. 7a) and interrupted (Fig. 7b), mainly owing to the decreased gas content and sound-wave reflection in the subpleural alveoli and interstitial lesions. Multiple small patchy consolidations were observed in the subpleural lesion (Fig. 8a), as was strip consolidation (Fig. 8b, 8c). The echogenicity in the lesions was homogeneous or inhomogeneous, and air bronchogram sign was visible, mostly in early and progressive stages (Fig. 8c). Because secondary pulmonary lobules were involved through interstitial inflammation, the interstitial tissues were thickened and swollen. Some bronchioles and alveoli were not involved because of high gas content and presented air bronchogram sign, visible in severe cases or local consolidation, possibly because local inflammation storm caused the consolidation and edema of most bronchioles and alveoli, and only large bronchi and part of the alveoli were not involved, as shown in Figure 9 by diffuse B-lines.

Color Doppler flow imaging showed a lack of blood flow signals in subpleural consolidation (Figs. 8a, 10). Use of different ultrasound scanners showed the blood flow signal to be weak, possibly owing to the pathologic changes unique to COVID-19 lesions. Signs of weak or absent blood flow, if confirmed by future studies, could be important biomarkers for COVID-19. In general, pulmonary consolidation caused by common inflammation is expected to show abundant blood flow, indicating good prognosis (Terslev et al. 2003). In contrast to the expectations of increased blood flow observed during common inflammation, weak blood flow is observed with COVID-19, which is known to progress rapidly and may cause death. Whether lung tissues are unable to quickly establish microvessel exchange mechanisms has yet to be further studied, but the ability of color Doppler ultrasound to detect the blood supply in consolidations more effectively than other imaging methods could make it an ideal imaging method for identifying potential markers to predict the prognosis in the early stage of the disease.

Peng et al. (2020) report LUS studies of pneumonia in 20 cases of confirmed COVID-19. Their findings are consistent with those of the earlier study (Huang et al. 2020). Although the article does not provide details of the scanning protocol or the imaging systems used, the LUS patterns were observed across a continuum from a mild alveolar interstitial pattern to a severe bilateral interstitial pattern to

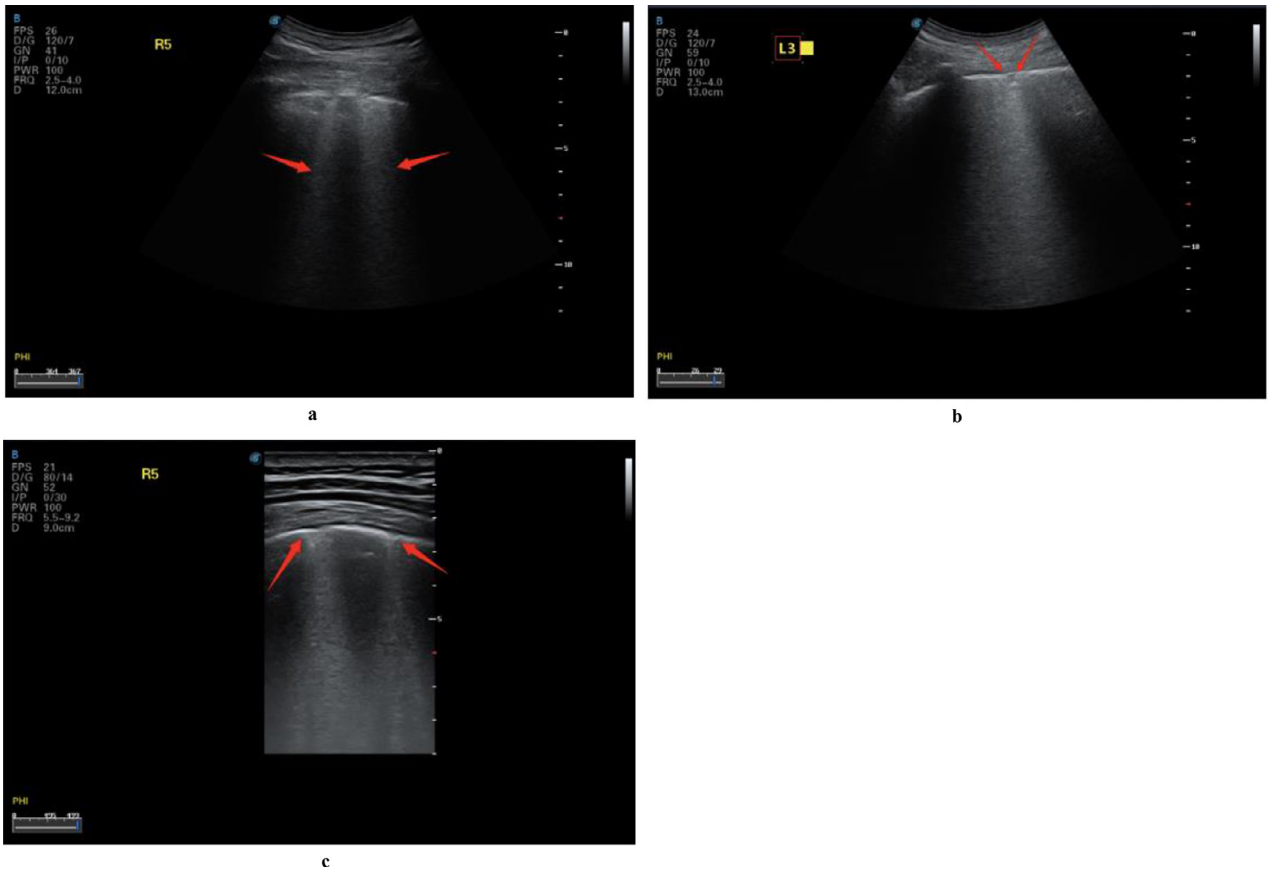

Fig. 6. Lung ultrasound images of multiple COVID-19 cases demonstrating different patterns of B-lines. (a) B-lines and waterfall sign in the right posterior upper area (*red arrow*), with an unsmooth pleural line. (b) The pleural line in the right posterior lower area is unsmooth and thin, with diffused B-lines and white-lung sign; A-lines have disappeared. (c) B-lines in the left posterior lower area, with A-lines having disappeared; small patchy lesions are observed, and the pleural line is discontinuous (*red arrow*). Reprinted with permission from Huang et al. (2020).

lung consolidation. Characteristic findings included thickening of the pleural line with pleural-line irregularity; B-lines in a variety of patterns including focal, multifocal and confluent; and consolidations in a variety of patterns including multifocal small, non-translobar and translobar with occasional mobile air bronchograms.

COVID-19 experience from Europe

Findings from patients have been reported from Europe as COVID-19 spread. A study from Italy (Lomoro et al. 2020) provides an overview of multimodality lung imaging findings in patients with COVID-19 pneumonia. LUS was performed in 22 patients from a total of 58. LUS showed thickened pleural lines and B-lines organized in different patterns (focal, multifocal and confluent) with a bilateral distribution. Patchy consolidations were observed in some cases. LUS findings demonstrated an association with CT findings such as ground-glass opacities and consolidations.

A study from northern Italy reports LUS findings from 12 patients admitted to a hospital with flu-like symptoms (Poggiali et al. 2020). Two patients had emphysema but without need of oxygen therapy at home; none of the patients had severe respiratory distress (partial pressure of arterial oxygen−fractional inspired oxygen ratio = 257−376 mm Hg). LUS findings showed irregular pleural lines with small subpleural consolidations, areas of white lung and thick, confluents and irregular vertical artifacts (B-lines). Spared areas were present bilaterally, mixed with pathologic areas. Only three patients had posterior subpleural consolidations.

Soldati et al. (2020) report findings from two patients from Italy with symptoms of intermediate pneumonia. Using a convex transducer, the lungs were scanned in 16 regions: anterior midclavicular (apical, medial and basal), right and left; posterior paraspinal (apical, medial and basal), right and left; and lateral axillary (apical and basal), medial right and left. Results showed early pulmonary manifestations represented by a patchy distribution of interstitial artifactual signs (single or confluent vertical artifacts, small white-lung regions). With the progress of infection, these patterns extend to

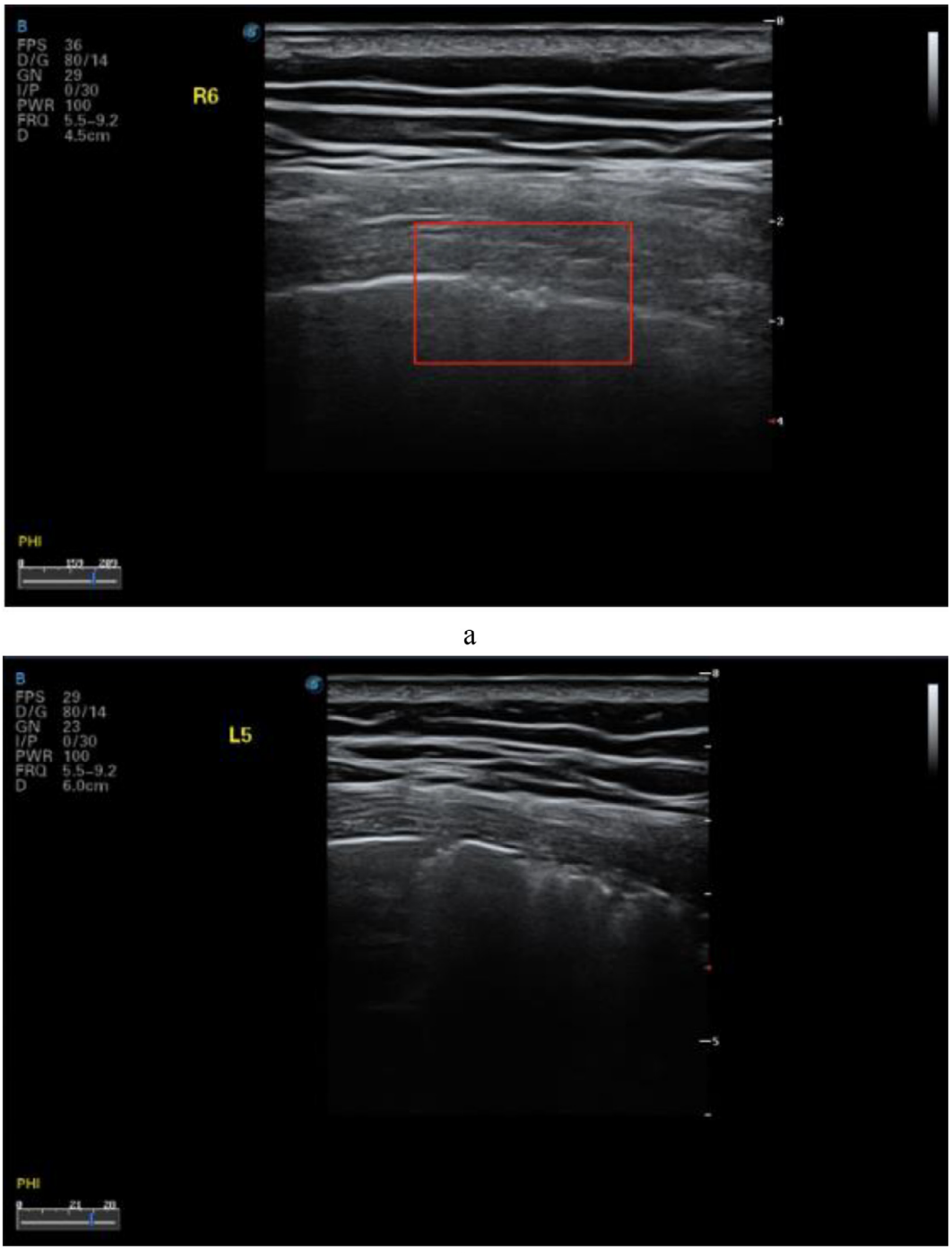

Fig. 7. Lung ultrasound images for confirmed COVID-19 cases obtained with a linear-array probe showing pleural-line irregularities. (a) The local pleural line in the right posterior lower area is unsmooth and the roughness is discontinuous. (b) The pleural line in the left posterior upper area is interrupted and discontinuous. Reprinted with permission from Huang et al. (2020).

multiple areas of the lung surface. The further evolution of lung abnormality (inflammation) presents as a patchy appearance of small subpleural consolidation with associated areas of white lung.

Buonsenso et al. (2020a) report a LUS study of a 52-year-old Italian man with documented COVID-19 infection. He was admitted to the emergency department with fever, cough, asthenia, headache, myalgia and

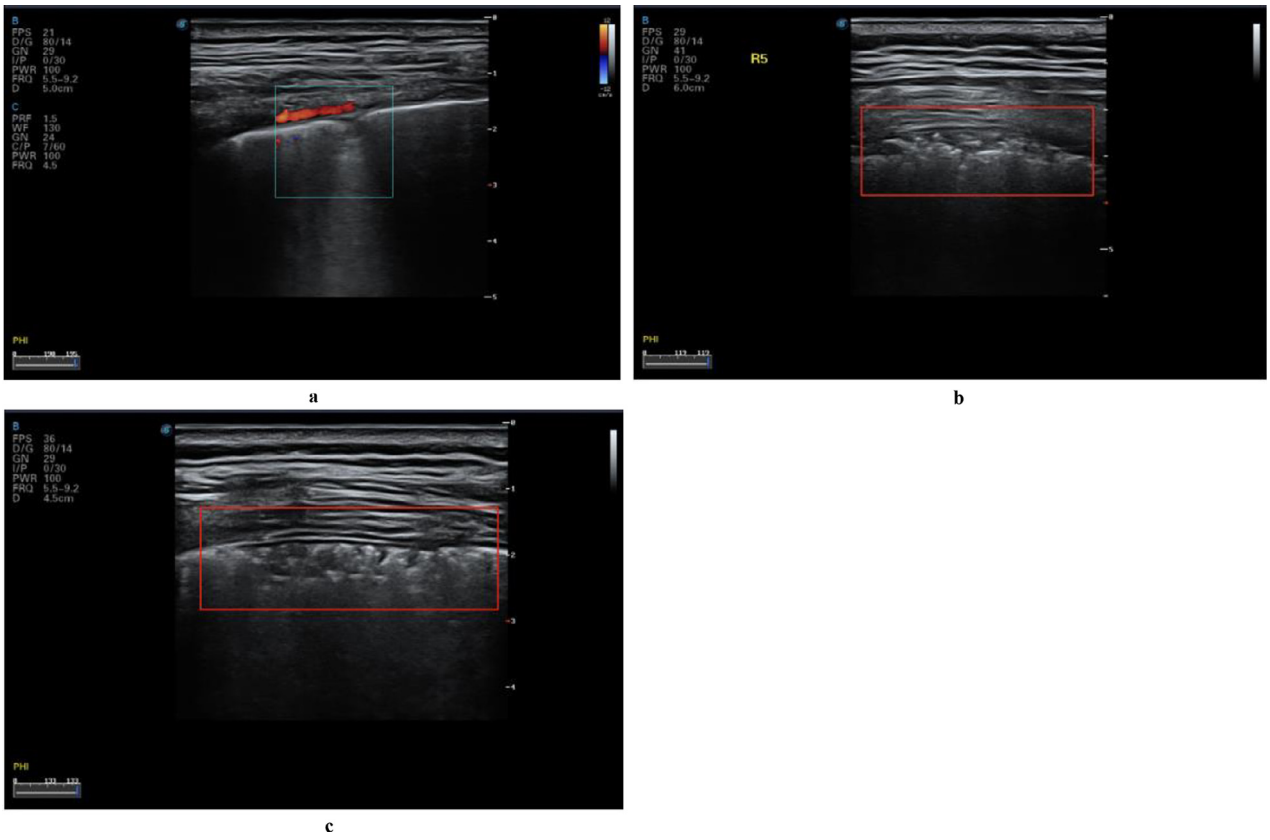

Fig. 8. Lung ultrasound images acquired using a linear-array probe. (a) Interrupted pleural line and patchy consolidation in the left posterior lower area, with fixed B-lines. The origin point is round and dull, and the subpleural area thickened. Color Doppler flow imaging shows no blood flow signal. (b) The pleural line in the right posterior upper area is interrupted and disappears. There is an air bronchogram sign in the strip and faint consolidation, and the connecting surface of the lung tissues is rough and unsmooth, with B-lines. (c) Discontinuous pleural line in the right posterior lower area and strip consolidation and air bronchogram sign, with a large number of B-lines. Reprinted with permission from Huang et al. (2020).

photophobia for 1 wk. The patient denied any travel during the prior month but reported a history of contact with several Chinese people (none with documented COVID-19 infection) and Italian people from the city of Bergamo, considered a high-risk area for COVID-19 infection. His on-air oxygen saturation was 90% and low-flow oxygen therapy was started. The patient was evaluated with a portable LUS performed with a 3.5 MHz convex probe. The portable device was used to minimize the risk of contamination and subsequent nosocomial spread despite its lower-quality images compared with more advanced ultrasound imaging systems. The thorax was scanned at bedside using the 12-lung-area approach: anterior superior and inferior, lateral superior and inferior and posterior superior and inferior, all bilaterally. Lung ultrasound examination clearly documented signs of interstitial-alveolar damage with bilateral, diffuse pleural-line abnormalities, subpleural consolidations, white-lung areas and thick, irregular vertical artifacts (B-lines). Spared areas were present bilaterally, mixed with pathologic areas. In addition, the researchers report a control case, imaged with the same device using the same ultrasound settings, performed during the same emergency department shift on a 38-y-old woman with high-grade fever, diffuse muscle and joint pain and cough, coming from a high-burden coronavirus area in northern Italy, who eventually tested negative for COVID-19. Lung ultrasound showed a normal pleural line with A-lines regularly reverberating and only one, regular vertical artifact (B-line) noted in a single area.

In another report by Buonsenso et al. (2020b), LUS findings were evaluated in four pregnant women who were confirmed to have COVID-19. The four women showed ultrasound features indicative of COVID-19 pneumonia at admission, including irregular pleural lines and vertical artifacts (B-lines) in all four cases and patchy areas of white lung in two cases. Three patients had resolution of lung pathology at ultrasound after 96 h of admission. Two pregnancies were ongoing, whereas two patients had cesarean delivery with no fetal complications.

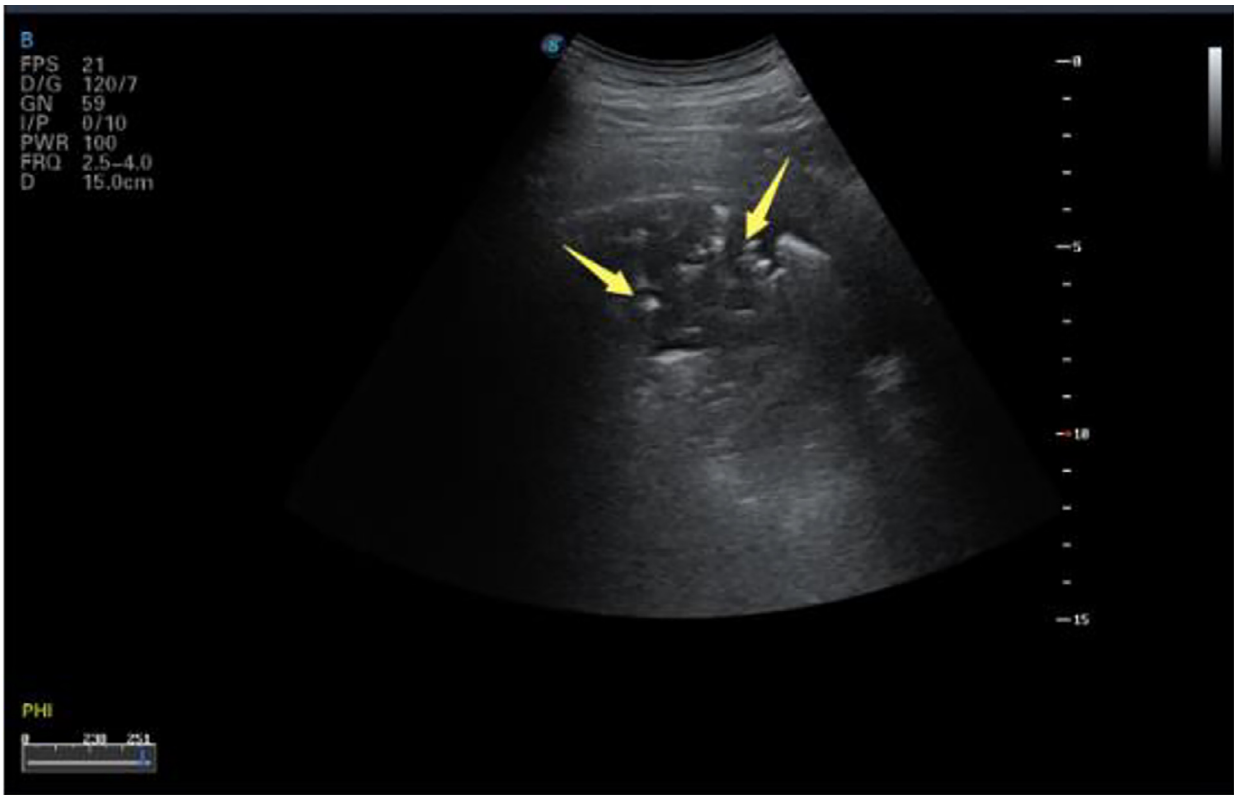

Fig. 9. Lung ultrasound image for confirmed COVID-19 patient scanned with a convex-array probe showing large areas of consolidation in the right posterior upper area and air bronchogram sign (*yellow arrow*). The pleural line is interrupted. Reprinted with permission from Huang et al. (2020).

Another team from Italy reports their experience with LUS findings in a pregnant woman diagnosed with COVID-19 (Inchingolo et al. 2020). Typical ultrasound features of this pulmonary pathology, including diffuse hyperechoic vertical artifacts (B-lines) with thickened pleural line and white lung with patchy distribution, were observed.

There is a report from Europe of personal experience using easily accessible portable ultrasound, from an emergency medicine physician in Spain who was infected while treating patients with COVID-19 [Tung-Chen Y 2020]. The investigator, a 35-year-old man, reported the day-by-day evolution of the disease evaluated by LUS (Fig. 11). LUS showed thickening in the pleural lines at the beginning, which progressed to the formation of basal B-lines in the next few days. Over time, subpleural consolidations started to appear and spread bilaterally on both posterior lower lobes in LUS.

COVID-19 experience from Japan

A group from Japan reports LUS findings from 10 confirmed cases of COVID-19 (Yasukawa and Minami 2020). Consistent with findings already described, the presence of characteristic findings of a diffuse B-line pattern, thick irregular pleural lines, confluent B lines and subpleural consolidation are reported. The findings of multiple B-lines correlated with the ground-glass areas on CT and in turn a high-degree interstitial syndrome. Small subpleural consolidations were observed in five patients only, and large consolidations in only one.

Individual COVID-19 cases reported from Canada and Turkey

Only one case has been reported from North America, from Canada (Thomas et al. 2020). Lung ultrasound of a 64-year-old female health care worker with no travel history, on day 10 after symptom onset, showed pleural thickening, subpleural consolidation and multifocal B-lines.

The latest case report is from Turkey (Kalafat et al. 2020): a 32-year-old pregnant woman in her 35th week who tested positive for COVID-19. LUS findings were consistent with viral pneumonia, with diffuse, thick B-lines bilaterally and predominantly basal posterior lung involvement. The anterior segment of the right upper lobe did not show marked involvement, and A-lines

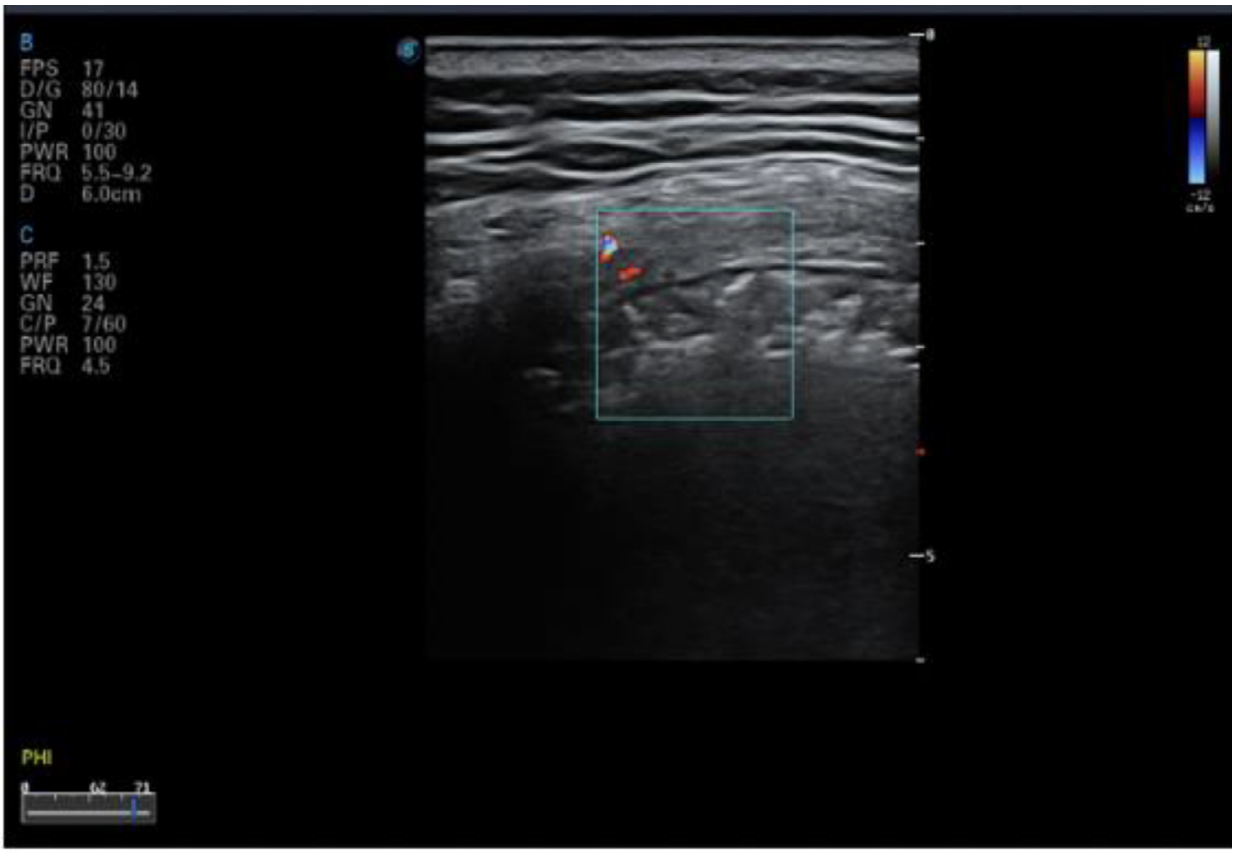

Fig. 10. Color Doppler ultrasound image for confirmed COVID-19 case showing no blood flow signal in the peri-pulmonary consolidation of the left posterior upper area, a significantly different finding from that of common inflammatory bacterial pneumonia. Reprinted with permission from Huang et al. (2020).

were visible on ultrasound. Chest CT findings correlated closely with those from LUS.

LUS findings in children with COVID-19

Two studies from Italy report LUS findings in children diagnosed with COVID-19. Mussolino et al. (2020) report LUS features of 10 consecutively admitted children with COVID-19 in two tertiary-level pediatric hospitals in Rome. LUS revealed signs of lung involvement during COVID-19 infection. In particular, vertical artifacts (B-lines), areas of white lung and subpleural consolidations and pleural irregularities were the main findings in pediatric COVID-19 pneumonia. LUS was found to be an important tool in moderate to severe pneumonia.

Denina et al. (2020) evaluated eight children younger than 17 y documented with COVID-19 who were admitted to the pediatric infections-diseases department. LUS documented confluent B-lines in half of the children and subpleural consolidations in two. Ultrasound findings were found to be in concordance with chest X-ray in all cases except one who had normal chest radiography.

CORRELATION OF LUS COVID-19 FINDINGS WITH CHEST CT SCAN

Comparison between LUS and chest CT scan on the same patients shows a strong correlation between the two imaging modes (Huang et al. 2020; Peng et al. 2020). The sensitivity and accuracy of LUS features are comparable with those of CT scan. Table 2 summarizes the features observed in LUS and the corresponding findings on chest CT scan. CT scans show patchy or confluent patterns, appearing with ground-glass opacity or mixed consolidative and ground-glass patterns; 10% of lesions have a “crazy paving” appearance. The diagnoses made from the two image modalities are highly consistent, but CT shows clearer and complete intra-pulmonary and apical lesions. Similar to CT, ground-glass opacity, nodule shadow, consolidation shadow and air bronchogram signs are observed in ultrasound images. However, CT has been found to be inferior to ultrasound in showing the smaller peri-pulmonary lesions and pleural and peri-pulmonary effusion (Huang et al. 2020). Furthermore, the real-

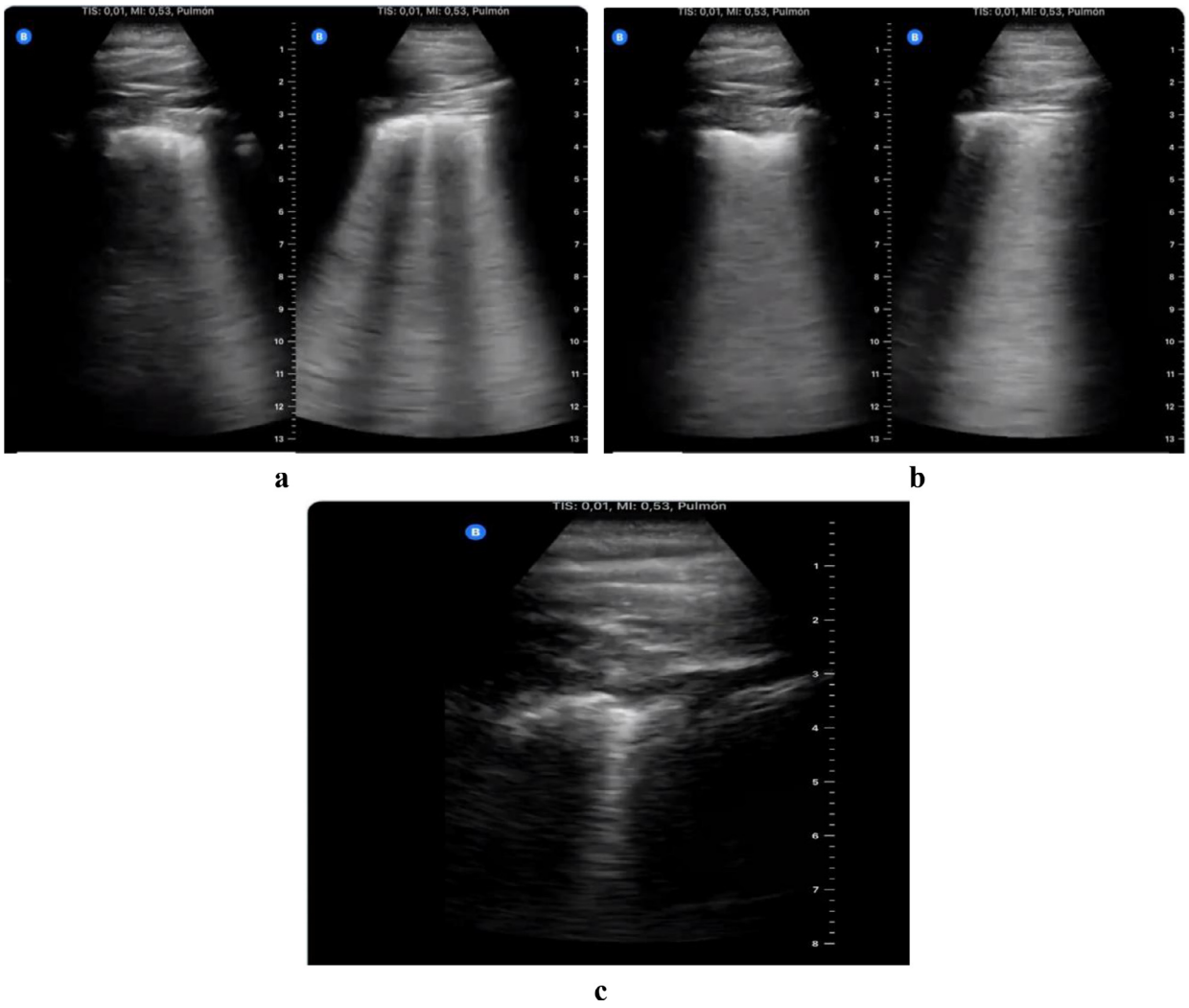

Fig. 11. Serial lung ultrasound images from a 35-y-old emergency physician who tested positive for COVID-19. (a) Scattered B-lines in both lungs, with thickened pleural line, at an early stage of the disease. (b) Diffused B-lines (white-lung sign) with disease progression. (c) Subsequent subpleural consolidation in a later stage of the disease. Reprinted with permission from Tung-Chen (2020).

time and dynamic nature of ultrasound imaging is found to be advantageous in distinguishing interstitial lesions and visualizing the distribution of blood flow and angiogenesis in inflammatory lesions.

A recognized limitation of lung ultrasonography is that it cannot detect lesions that are deep within the lung, as aerated lung blocks the transmission of ultrasound (*i. e.,* the abnormality must extend to the pleural surface to be visible on ultrasonography examination). Chest CT is required to detect pneumonia that does not extend to the pleural surface.

CONCLUSIONS AND FUTURE DEVELOPMENTS

Despite the early advent of disease and the fact that image findings are still evolving, the early experience from LUS use in COVID-19 cases is promising. Nearly all the studies using LUS for imaging with COVID-19 patients report that characteristic ultrasound findings can be used to help physicians detect and stage the disease and track its progression. The common patterns observed by the studies include bilateral and posterobasal predominance and multiple B-lines ranging from focal to diffuse, with spared areas representing thickened subpleural inter-lobular septa. Irregular, thickened pleural lines with scattered discontinuities are commonly seen in the images. Subpleural consolidations can be associated with a discrete, localized pleural effusion. Color Doppler imaging shows inflammatory lesions to be relatively avascular. Alveolar consolidation having a tissue-like appearance, with dynamic and static air bronchograms, is often associated with severe, progressive

Table 2. Lung ultrasound (LUS) features and corresponding chest computed tomography (CT) findings in patients with COVID-19

LUS	Chest CT
Thickened pleural line	Thickened pleura
B-lines (multifocal, discrete or confluent)	Ground-glass shadowing
Confluent B-lines	Pulmonary infiltrating shadowing
Small consolidations	Subpleural consolidation
Both non-translobar and translobar consolidation	Translobar consolidation
Pleural effusion rare	Pleural effusion rare
Multilobar distribution of abnormalities	More than two lobes affected
Early stages: Focal B-lines and pleural-line thickening	Early stages: Negative or atypical findings
Progressive and late stages: Confluent B-lines, pleural-line thickening, then small consolidation which progress to lobar consolidation	Progressive and late stages: Diffuse scattered or ground-glass shadow which progresses to lung consolidation

disease. Restored aeration and reappearance of bilateral A-lines during recovery have been reported. Collectively, identification of these characteristic patterns can improve the specificity of LUS for imaging COVID-19 lung changes.

While the results to date are encouraging, future studies optimizing the use of LUS will be helpful. This could include the use of a standardized lexicon for ultrasound features for classification of COVID-19 LUS, similar to those described in other areas of sonography of breast, liver and thyroid cancers. Using such a lexicon can add objectivity to LUS features in differentiating COVID-19 from other diseases by the presence or absence of characteristic ultrasound features. Adding new features involving blood flow characteristics by Doppler ultrasound and viscoelastic properties by elastography (Zhang et al. 2011) could also enhance diagnosis.

Further improvements in the diagnostic performance of LUS for COVID-19 can be achieved by combining advanced image analysis of LUS features with computer-aided diagnosis by machine learning. Establishment of a large, representative imaging data set with contributions from multiple facilities will be needed for training and testing computer mod When trained on enough data, machine-learning models often increase confidence in diagnosis, especially in low-resource communities around the globe that lack experience in LUS.

Acknowledgments—The authors would like to thank Theodore W. Cary for his substantial contribution in reading and editing the manuscript.

Conflict of interest disclosure—The authors declare no competing interests.

REFERENCES

Aldrich JE. Basic physics of ultrasound imaging. Crit Care Med 2007;35 (5 Suppl):S131–S137. doi: 10.1097/01.CCM.0000260624.99430.22.

Arbelot C, Dexheimer Neto FL, Gao Y, Brisson H, Chunyao W, Lv J, Valente Barbas CS, Perbet S, Prior Caltabellotta F, Gay F, Deransy R, Lima EJS, Cebey A, Monsel A, Neves J, Zhang M, Bin D, An Y, Malbouisson L, Salluh J, Constantin JM, Rouby JJ, Biestro A, Vezinet C, Garçon P, El Hadj Kacem N, Lemesle D, Lucena B, de Paula Pinto Schettino G, Cristovao D, de Tarso Roth Dalcin P, Carmona MJC. Lung ultrasound in emergency and critically ill patients: Number of supervised exams to reach basic competence. Anesthesiology 2020;899–907 NN.

Bakhru RN, Schweickert WD. Intensive care ultrasound: I. Physics, equipment, and image quality. Ann Am Thorac Soc 2013;10:540–548.

Bouhemad B, Zhang M, Lu Q, Rouby JJ. Clinical review: Bedside lung ultrasound in critical care practice. Crit Care 2007;11:205.

Buonsenso D, Piano A, Raffaelli F, Bonadia N, de Gaetano Donati K, Franceschi F. Point-of-care lung ultrasound findings in novel coronavirus disease-19 pnemoniae: A case report and potential applications during COVID-19 outbreak. Eur Rev Med Pharmacol Sci 2020a;24:2776–2780.

Buonsenso D, Raffaelli F, Tamburrini E, et al. Clinical role of lung ultrasound for the diagnosis and monitoring of COVID-19 pneumonia in pregnant women. Ultrasound Obstet Gynecol 2020;. doi: 10.1002/uog.22055 [published online ahead of print, 2020 Apr 26].

Denina M, Scolfaro C, Silvestro E, et al. Lung Ultrasound in Children With COVID-19 [published online ahead of print, 2020 Apr 21]. Pediatrics 2020; e20201157. doi: 10.1542/peds.2020-1157.

Dietrich CF, Mathis G, Blaivas M, Volpicelli G, Seibel A, Wastl D, Atkinson NSS, Cui XW, Fan M, Yi D. Lung B-line artefacts and their use. J Thorac Dis 2016;8:1356–1365.

Huang Y, Wang S, Liu Y, Zhang Y, Zheng C, Zheng Y, Zhang C, Min W, Zhou H, Yu M, Hu M. A preliminary study on the ultrasonic manifestations of peripulmonary lesions of non-critical novel coronavirus pneumonia (COVID-19). SSRN Electron J 2020; (February 26, 2020). Available at SSRN: https://ssrn.com/abstract=3544750 or http://dx.doi.org/10.2139/ssrn.3544750.

Hui DS, I Azhar E, Madani TA, Ntoumi F, Kock R, Dar O, Ippolito G, Mchugh TD, Memish ZA, Drosten C, Zumla A, Petersen E. The continuing 2019-nCoV epidemic threat of novel coronaviruses to global health—the latest 2019 novel coronavirus outbreak in Wuhan, China. Int J Infect Dis 2020;91:264–266.

Inchingolo R, Smargiassi A, Moro F, et al. The Diagnosis of Pneumonia in a Pregnant Woman with COVID-19 Using Maternal Lung Ultrasound. Am J Obstet Gynecol 2020;. doi: 10.1016/j.ajog.2020.04.020 S0002-9378(20)30468-3. [published online ahead of print, 2020 Apr 28] Accessed.

Kalafat E, Yaprak E, Cinar G, Varli B, Ozisik S, Uzun C, Azap A, Koc A. Lung ultrasound and computed tomographic findings in pregnant woman with COVID-19. Ultrasound Obstet Gynecol 2020;55:835–837.

Koegelenberg CFN, Von Groote-Bidlingmaier F, Bolliger CT. Transthoracic ultrasonography for the respiratory physician. Respiration 2012;84:337–350.

Li K, Fang Y, Li W, et al. CT image visual quantitative evaluation and clinical classification of coronavirus disease (COVID-19) [e-pub ahead of print]. Eur Radiol 2020;. doi: 10.1007/s00330-020-06817-6 [published online ahead of print, 2020 Mar 25]. Accessed.

Li X, Zeng W, Li X, Chen H, Shi L, Li X, Xiang H, Cao Y, Chen H, Liu C, Wang J. CT imaging changes of corona virus disease 2019 (COVID-19): A multi-center study in Southwest China. J Transl Med 2020b;18:154.

Lichtenstein D, Malbrain MLNG. Lung ultrasound in the critically ill (LUCI): A translational discipline. Anaesthesiol Intensive Ther 2017;49:430–436.

Lichtenstein DA, Mezière GA. Relevance of lung ultrasound in the diagnosis of acute respiratory failure: The BLUE protocol. Chest 2008;134:117–125.

Lichtenstein DA, Mezière GA, Lagoueyte JF, Biderman P, Goldstein I, Gepner A. A-lines and B-lines: Lung ultrasound as a bedside tool for predicting pulmonary artery occlusion pressure in the critically ill. Chest 2009;136:1014–1020.

Lomoro P, Verde F, Zerboni F, Simonetti I, Borghi C, Fachinetti C, Natalizi A, Martegani A. COVID-19 pneumonia manifestations at the admission on chest ultrasound, radiographs, and CT: Single-center study and comprehensive radiologic literature review. Eur J Radiol Open 2020;7 100231.

Miller A. Practical approach to lung ultrasound. BJA Educ 2016;16:39–45.

Musolino AM, Supino MC, Buonsenso D, et al. Lung Ultrasound in Children with COVID-19: Preliminary Findings [published online ahead of print, 2020 May 3]. Ultrasound Med Biol. 2020;. doi: 10.1016/j.ultrasmedbio.2020.04.026 S0301-5629(20)30198-8.

Peng QY, Wang XT, Zhang LN. Findings of lung ultrasonography of novel corona virus pneumonia during the 2019−2020 epidemic. Intensive Care Med 2020;46:849–850.

Poggiali E, Dacrema A, Bastoni D, Tinelli V, Demichele E, Mateo Ramos P, Marcianò T, Silva M, Vercelli A, Magnacavallo A. Can lung US help critical care clinicians in the early diagnosis of novel coronavirus (COVID-19) pneumonia?. Radiology 2020; NN:200847.

Chen H, Ai L, Lu H, Li H. Clinical and imaging features of COVID-19 [published online ahead of print, 2020 Apr 27]. Radiol Infect Dis 2020;. doi: 10.1016/j.jrid.2020.04.003 10.1016/j.jrid.2020.04.003.

Van Doremalen Neeltje, Bushmaker Trenton, Morris Dylan H, Holbrook Myndi G, Gamble Amandine, Williamson Brandi N, Tamin Azaibi, Harcourt Jennifer L, Thornburg Natalie J, Gerber Susan I, Lloyd-Smith James O, de Wit Emmie, Munster Vincent J. Aerosol and Surface Stability of SARS-CoV-2 as Compared with SARS-CoV-1. New England Journal of Medicine 2020;. doi: 10.1056/NEJMc2004973.

Saraogi A. Lung ultrasound: Present and future. Lung India 2015;32:250–257.

Soldati G, Smargiassi A, Inchingolo R, et al. Is There a Role for Lung Ultrasound During the COVID-19 Pandemic? [published online ahead of print, 2020 Mar 20]. J Ultrasound Med 2020;. doi: 10.1002/jum.15284 10.1002/jum.15284.

Terslev L, Torp-Pedersen S, Qvistgaard E, Danneskiold-Samsoe B, Bliddal H. Estimation of inflammation by Doppler ultrasound: Quantitative changes after intra-articular treatment in rheumatoid arthritis. Ann Rheum Dis 2003;62:1049–1053.

Thomas A, Haljan G, Mitra A. Lung ultrasound findings in a 64-year-old woman with COVID-19. Can Med Assoc J 2020;192(15):E399.

Tung-Chen Y. Yale Tung Chen (@yaletung) / Twitter. 2020; https://twitter.com/yaletung?ref_src=twsrc%5Egoogle%7Ctwcamp%5Eserp%7Ctwgr%5Eauthor.

Velavan TP, Meyer CG. The COVID-19 epidemic. Trop Med Int Health 2020;25:278–280.

Wang K, Kang S, Tian R, Zhang X, Wang Y. Imaging manifestations and diagnostic value of chest CT of coronavirus disease 2019 (COVID-19) in the Xiaogan area. Clin Radiol 2020;75:341–347.

Wong HYF, Lam HYS, Fong AHT, Leung ST, Chin TWY, Lo CSY, Lui MM-S, Lee JCY, Chiu KWH, Chung T, Lee EYP, Wan EYF, Hung FNI, Lam TPW, Kuo M, Ng MY. Frequency and distribution of chest radiographic findings in COVID-19 positive patients. Radiology 2019; 201160.

World Health Organization. Naming the coronavirus disease (COVID-19) and the virus that causes it. World Health Organization 2020;1. https://www.who.int/emergencies/diseases/novel-coronavirus-2019/technical-guidance/naming-the-coronavirus-disease-(covid-2019)-and-the-virus-that-causes-it.

World Health Organization. WHO director-general's opening remarks at the media briefing on COVID-19—11 March 2020. : WHO Dir. Gen. speeches.; 2020. p. 4. https://www.who.int/dg/speeches/detail/who-director-general-s-opening-remarks-at-the-media-briefing-on-covid-19—11-march-2020.

Yang X, Yu Y, Xu J, Shu H, Xia J, Liu H, Wu Y, Zhang L, Yu Z, Fang M, Yu T, Wang Y, Pan S, Zou X, Yuan S, Shang Y. Clinical course and outcomes of critically ill patients with SARS-CoV-2 pneumonia in Wuhan, China: A single-centered, retrospective, observational study. Lancet Respir Med 2020;2600:1–7.

Yasukawa K, Minami T. Point-of-Care Lung Ultrasound Findings in Patients with COVID-19 Pneumonia. Am J Trop Med Hyg 2020;102(6):1198–1202. doi: 10.4269/ajtmh.20-0280.

Zhang X, Qiang B, Hubmayr RD, Urban MW, Kinnick R, Greenleaf JF. Noninvasive ultrasound image guided surface wave method for measuring the wave speed and estimating the elasticity of lungs: A feasibility study. Ultrasonics 2011;3:289–295.

Zieleskiewicz L, Lagier D, Contargyris C, Bourgoin A, Gavage L, Martin C, Leone M. Lung ultrasound-guided management of acute breathlessness during pregnancy. Anaesthesia 2013;68:97–101.